

Influence of heat treatments on the fatigue strength performance of low carbon steels

C. G. Cárdenas-Arias¹, C. L. Sandoval-Rodríguez², A. D. Rincon-Quintero^{1,4} and O. Lengerke³

¹ Research Group on Design and Materials – DIMAT, Unidades Tecnológicas de Santander, Bucaramanga, Colombia

² Research group on energy systems, automation and control - GISEAC, Unidades Tecnológicas de Santander, Bucaramanga, Colombia

³ Advanced Control Research Group-GICAV, Unidades Tecnológicas de Santander, Bucaramanga, Colombia

⁴ Departamento de Ingeniería Energética, Universidad del País Vasco, Bilbao, España

*Corresponding author E-mail: ccardenas@correo.uts.edu.co

ABSTRACT

In this research work, the behavior of low-carbon steels is studied, taking as a reference the AISI SAE 1020 steel and the influence of heat treatments on fatigue resistance performance. Fatigue tests were performed under rotary bending conditions on Moore's machine, where 24 samples calibrated to a half-inch diameter were broken. The specimens were machined in accordance with the ASTM E-606 standard, which were classified into three groups with special characteristics, of 8 samples each, where the first group is composed of specimens without heat treatment, the second group are specimens with quenching and the last group of specimens with quenching and tempering; in the same way, 4 different weights were used, taking into account that the specimens were in the finite life zone with high cycling, and with this data the Wholer S-N curve was constructed. The curves construction of agreement to the data thrown in the tests concluded that the specimens with tempering treatment weaken the material compared to those that have tempering treatment since this improves the property when applying large loads and when it approaches A finite life tends to behave like a material without treatment.

Keywords: Fatigue, rotary bending, S-N curve, heat treatments

1. Introduction

Since 1850, it has been recognized that a metal subjected to repeated or fluctuating stresses will fail at a stress much lower than that required to fracture under a single load application. These types of failures, occurring under dynamic conditions and over long periods of service, became known as fatigue failures [1]. Subsequently, the study of the fatigue fracture mechanism has been developed with great intensity and it has now been stated that 90% of all fractures in services are due to the fatigue mechanism [2],[3]–[7]. It is important to consider that notches in parts significantly reduce the fatigue resistance of steels, sometimes reducing fatigue resistance to half or a quarter of the steel's strength. [8],[9],[10]. Fatigue fractures are accentuated when the parts are surface decarburized, but they tend to decrease when steel parts are case-hardened or nitrided, and also when they have been subjected to cold working of the surface that hardens the peripheral area. Fatigue has been extensively investigated in previous studies [11].

On the other hand, knowledge of materials science provides the necessary tools to understand the general behavior of some materials, in order to properly apply the principles of component selection [12],[13]–[17]. In theory, when calculating the resistance for affected specimens, it is suggested that heat treatments increase this resistance, affecting it positively [18],[19]–[23]. For this reason, it is necessary to study how steel acts by improving its mechanical properties. Based on this theory, it was decided to apply tempering heat treatment, which is performed routinely in industry and is carried out by hand. This involves uncertainty in the results, as it depends on the objectivity of the operator and the cooling condition [24],[25], [26]. Thus, a quench-temper process, also known as annealing, was performed. The main objective of this work is to present a series of results obtained from tests, which serve as a basis for illustrating the mechanical behavior of the influence of

heat treatments on fatigue in low-carbon steels. The S-N curve was constructed, allowing observation of the behavior under rotational bending fatigue conditions. The document consists of a theoretical framework, the methodology for conducting the research, the tests performed on the specimens, the results, and the conclusions of the work.

2. Methods: Research design

The methodology used in this work was experimental. A bibliographic review was conducted to document the research, an experimental design was developed to select the number of test specimens and provide experimental guidelines for compliance with the standard, and the status of the equipment used in the process, such as the heat treatment furnace and the machine for functional testing under rotary bending conditions or Moore machine, were verified. This was done to meet the objectives set out in this project as a tool for obtaining results and conclusions that allow comparison between similar studies.

2.1. Research stage

This phase allowed the evaluation and definition of the appropriate method for the heat treatment of the samples, which consisted of quenching and tempering. A fatigue test was then performed under rotary bending to determine the behavior of the AISI SAE 1020 steel.

This research is experimental, so bibliographic information on steel, heat treatments, and the fatigue resistance of AISI SAE 1020 steel was collected. Since the necessary data is obtained from observations and tests performed in the laboratory, the statistical results were recorded and processed in Excel. The results were also analyzed, documenting the information according to the proposed procedure and the technical requirements of the project and the equipment involved in the process.

2.2. Samples selection

Following the project requirements, AISI SAE 1020 steel was considered as the study material. 24 test specimen were built that comply with the ASTM E606 standard [27], taking into account the possibility of having three standard samples for different tests and fatigue test conditions.

Table 1. Composition of AISI SAE 1020 steel

Chemical composition	C %	Mn %	P max. %	S max. %	Si max. %
Typical analysis %	0.18 0.23	0.3 0.6	0.04	0.05	0.15 0.3

Delivery condition: Annealed
Delivery hardness: 150 – 190 HB

2.3. Experiment design

For the proper execution and development of the project, the implementation of an experimental model is necessary [28] to determine the number of specimens needed to increase the precision and validity of the experiment, determine the number of data and provide an estimate of experimental error, which becomes a basic unit for determining whether the observed differences in the data are statistically significant.

An experimental design was carried out that met the project requirements based on the ASTM E739 standard [29], analyzing the behavior of the E-N curve, the fatigue test with quenching and tempering, as well as the behavior of finite life in different heat treatments. The following specifications were taken into account when carrying out laboratory tests:

2.3.1. Temperature

For this procedure, the critical temperatures for AISI SAE1020 steel were used, see Table 2 [30]

Table 2. Critical temperatures for SAE 1020 steel, Adapted from: [30]

Steel	SAE 1020
Critical temperatures	A1 = 727°C A3 = 830 °C
Annealing process	727- (80 a 170) = 557°C a 647°C
Annealing	830+30 = 860°C
Normalized	830 + 55 = 885 °C

Figure 1 shows a continuous cooling transformation (CCT) diagram for a steel with 0.2% C, where when tempering is applied to SAE 1020 steel, a mixture of phases is obtained.

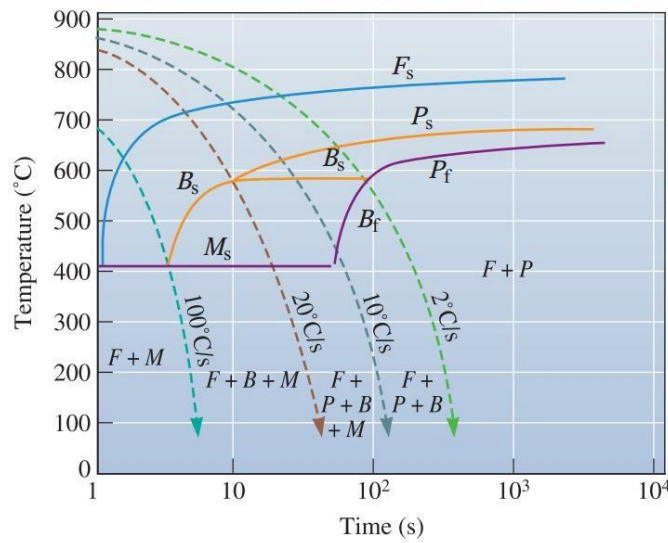


Figure 1. CCT diagram for low-carbon steels (Adapted from [30])

2.3.2. Quenched

To select the quenching substance for the hardening, it was taken into account that the specimens that are going to be subjected to fatigue have a diameter of 1/4” in their middle section. According to the Grossman graph Figure 2, for this diameter an H coefficient of 1 can be assumed, which would give a Jominy distance of approximately 1/32”, this coefficient is achieved by using water as the hardening medium without agitation [31].

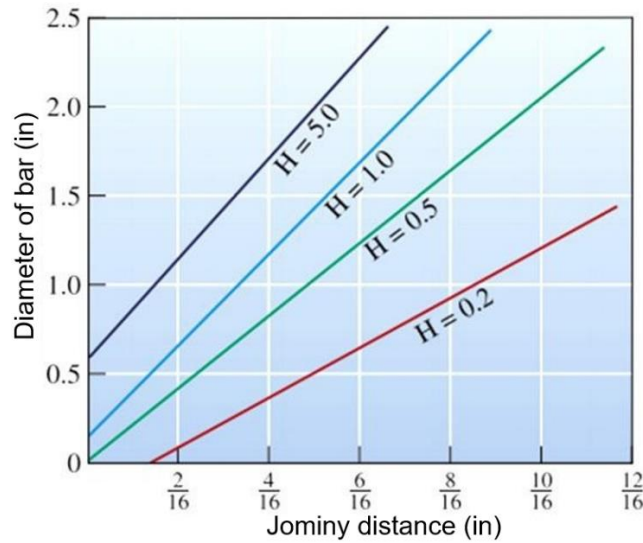


Figure 2. Grossman graph adapted from [30], [31]

Table 3. H coefficient of severity of quenched Adapted from [30]

Mean	H Coefficient	Cooling rate at the center of a 1 in. bar (°C/s)
Oil (not agitated)	0.25	18
Oil (agitated)	1.0	45
H2O (not agitated)	1.0	45
H2O (agitated)	4.0	190
Brine (not agitated)	2.0	90
Brine (agitated)	5.0	230

The hardness at the center of the test piece is obtained from figure 3, with the hardenability band for AISI SAE 1020 steel: Because the test piece has a small diameter, the maximum hardness will be obtained, which will be in the range 33-44 HRC [32].

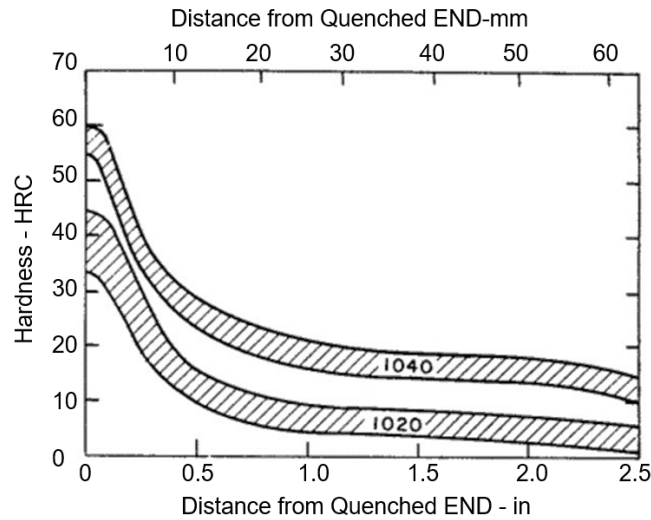


Figure 3. Hardness as a function of distance from the quenched end

Adapted from: Steel Casting Handbook, Supplement [32]

2.3.3. Tempering Process

This treatment is used to reduce the residual stresses generated during tempering, which changes the properties of the material and reduces its hardness [33]. To select the tempering temperature, Figure 4 is used, which shows the variation in hardness depending on the temperature selected for tempering. The decision was made to use a temperature of 350°C for the treatment since this will not cause a significant loss in hardness [34].

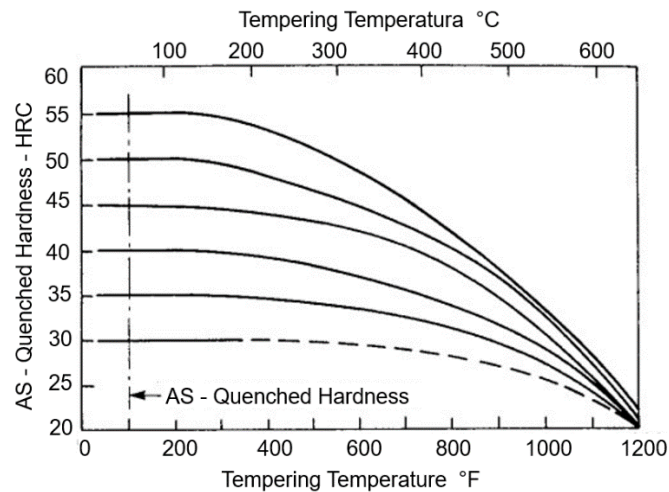


Figure 4. Hardness variation as a function of tempering temperature. Adapted from: [32] Steel Casting Handbook, "Final Treatment" Supplement

According to the above, a heat treatment was performed on 16 of the 24 test pieces made of AISI SAE 1020 steel, in quenched and tempered condition to evaluate the influence and performance of the resistance to fatigue by rotary bending and thus evaluate its behavior.

3. Statistical processing to validate the tests

Statistical processing of the data obtained from each test is based on ASTM E739, Standard Practice for Statistical Analysis of Linear or Linearized Stress-Life (S-N). According to the standard, linear behavior is assumed, and data processing is performed for a test with L levels and a total number of k samples, which helps generate a graph that expresses the material's behavior in a stress-versus-cycles curve.

3.1. Test specimen and definition of the number of samples

Based on ASTM E606 and ASTM E739 standards, 24 test pieces were manufactured to form three groups of eight specimens. Eight of these specimens were subjected to the quenching process and eight to quenching and tempering. The other eight specimens were left untreated to provide reference results.

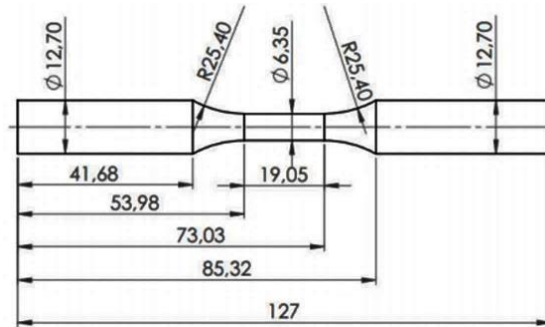


Figure 5. Prototype dimensions

3.2. Test development

After establishing the technical specifications and developing the statistical model that explains the calculations and graphs obtained during the process, the test pieces were constructed by turning and with a highly polished surface, to prevent the test piece from failing in a zone other than the one of interest and to consider the test valid for rotational bending fatigue. See figures 5, 6 and 7.



Figure 6. Constructed specimen

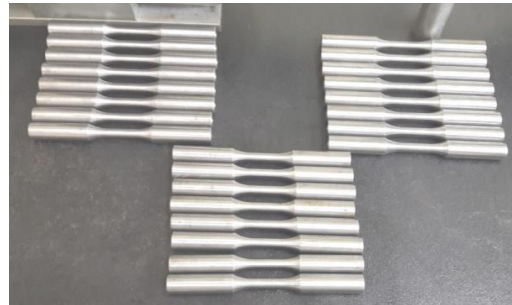


Figure 7. Test specimen without heat treatment

The samples were introduced into an electric furnace that allowed the treatment to develop properly Figure 8. The test pieces were subjected to an Austenitization temperature (A3), equivalent to 885 °C, for 1 hour.



Figure 8. Heat treatment furnace

After subjecting the 16 samples to the oven, they are tempered in still water as shown in figure 9, until reaching room temperature.



Figure 9. Water quenching of test specimens

When the test pieces reached room temperature, 8 test pieces were subjected to the annealing process, for which they were again subjected to heating at a temperature of 350°C for one hour as shown in Figure 10, and finally cooled to room temperature.



Figure 10. Test pieces with annealing treatment

In Figure 11, the 2 groups of test pieces can be seen after being exposed to the heat treatments of quenching and tempering, and an untreated test piece to be subjected to fatigue tests by rotary bending.



Figure 11. Test specimens after heat treatment

To perform the rotary bending fatigue tests, the Moore machine [35] was used, designed under the ASTM standard, which has different sensors that allow counting the revolutions given until the break time and a load cell that allows measuring the weight generated by the power screw. With these two variables it is possible to construct the stress versus cycle graph or Wholer dynamic stress diagram.

The machine has a ½ HP Siemens motor that generates the power needed to rotate the test piece at 1800 RPM, likewise the weights can be applied to each sample by means of the screw and this will be displayed on the Lexus brand screen, which is connected to the load cell, see Figure 12



Figure 12. Rotary bending fatigue machine.

To determine the cycles, a sensor was installed that counts the revolutions of the shaft and is connected to the PLC, where the data reading is displayed on the screen. This sensor shuts off the motor when the test specimen breaks and then indicates when the motor stops. It has two sensors or pilot lights: one red that indicates the motor is stopped and one green that indicates it is running. See figure 13.



Figure 13. Load cell and PLC screen



Figure 14. Broken test specimen

With the values obtained in the different tests, the S-N curves were made for each of the groups of 8 test pieces, the first group of test pieces without any treatment, the second group of test pieces with hardening treatment and the third group with annealing treatment.

4. Results and discussion

The load data (kg), N (cycles) and S (Mpa) obtained in the rotational bending fatigue tests of the 8 untreated specimens are presented below, see Table 4.

Table 4. Rotational bending fatigue test results for untreated specimen

Test	Load [kg]	N (cycles)	Stress [Mpa]
1	18	254968	351.23
2	18	247590	351.23
3	20	177238	390.25
4	20	161975	390.25
5	22	122547	429.28
6	22	115037	429.28
7	24	78333	468.31
8	24	80087	468.31

The load data (Kg), N (cycles) and S (Mpa), of the 8 specimens with tempering treatment and rotary bending fatigue test are presented in Table 5.

Table 5. Rotational bending fatigue test results for specimen with quenched

Test	Load [kg]	N (cycles)	Stress [Mpa]
1	18	145820	351,23
2	18	116564	351,23
3	20	86010	390,25
4	20	84166	390,25
5	22	55980	429,28
6	22	57409	429,28
7	24	34166	468,31
8	24	34153	468,31

The load data (Kg), N (cycles) and S (Mpa), obtained from the 8 test pieces with annealing treatment and rotary bending fatigue tests, are presented in Table 6.

Table 6. Results of the rotary bending fatigue test for the specimen with annealing treatment

Test	Load [kg]	N (cycles)	Stress [Mpa]
1	18	318342	351,23
2	18	329837	351,23
3	20	256789	390,25
4	20	239873	390,25
5	22	184345	429,28
6	22	178234	429,28
7	24	129873	468,31
8	24	132350	468,31

The curves show the fatigue behavior as a function of alternating stress, called S-N curves, for each of the conditions studied, without heat treatment, with quenching treatment and with annealing treatment, respectively. The linear regression models found, which are represented by the dashed lines, demonstrate that for the finite life interval, quenching heat treatment weakens the steel exposed to rotational fatigue at any point on the curve. It was also shown that the annealing heat treatment improves the fatigue property when applying large loads because when approaching finite life it tends to behave like an untreated material. As can be seen in Figure 15.

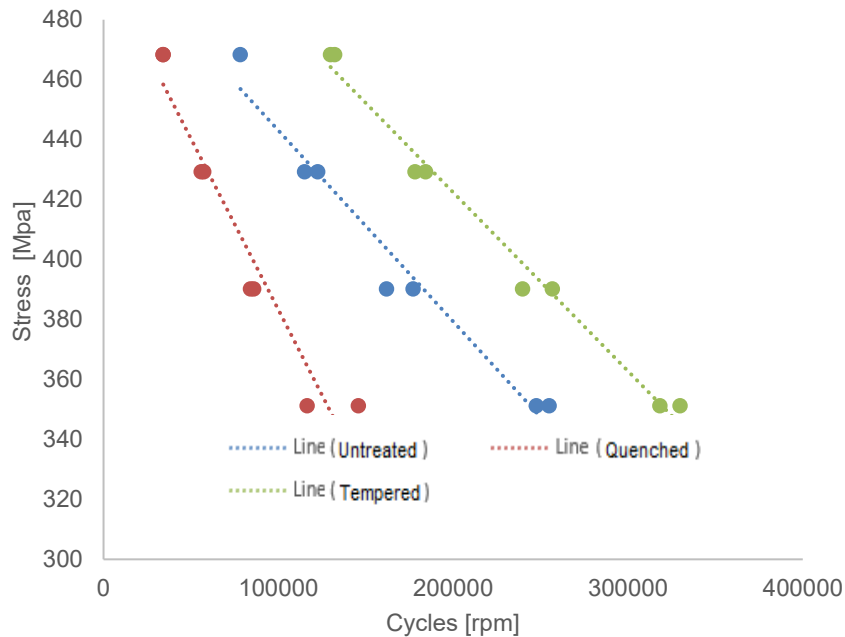


Figure 15. S-N diagram with different treatments

5. Conclusions

The results obtained from rotary bending fatigue tests on AISI SAE 1020 steel clearly demonstrate the effect of heat treatments on material strength under cyclic loading conditions. Contrary to the general theoretical expectation suggesting an improvement in strength with hardening, it was shown that this treatment decreases the steel's service life under fatigue stresses, reducing its performance by 2.56% compared to untreated specimens. This behavior may be associated with the microstructure generated during cooling and the induced residual stresses, suggesting the need for more rigorous control of the hardening process.

In contrast, the combined quenching and tempering treatment showed a significant improvement in fatigue strength, increasing the material's service life by 7.15%. This improvement is consistent with reports in the technical literature, where tempering acts by reducing the material's internal stresses and stabilizing its microstructure, without causing a significant loss of hardness. This demonstrates that properly applied tempering can be an effective strategy for extending the service life of components subjected to repetitive loading.

Finally, the research demonstrates that controlling heat treatment parameters and their proper application have a direct impact on the fatigue performance of low-carbon steels. It is recommended that additional microstructural studies be conducted and the number of specimens expanded to statistically validate these findings. It is also recommended that alternative treatments such as nitriding or case-hardening be explored to evaluate their comparative effect under similar conditions.

Declaration of competing interest

The authors declare that they have no known financial or non-financial competing interests in any material discussed in this paper.

Funding information

No funding was received from any financial organization to conduct this research.

Author contribution

The contribution to the paper is as follows: C. G. Cárdenas-Arias, C. L. Sandoval-Rodríguez: study conception and design; A. D. Rincon-Quintero: data collection; C. G. Cárdenas-Arias, C. L. Sandoval-Rodríguez and O. Lengerke: analysis and interpretation of results; C. G. Cárdenas-Arias, C. L. Sandoval-Rodríguez and A. D. Rincon-Quintero: draft preparation. All authors approved the final version of the manuscript.

References

- [1] S. Hernández Molina, “Estudio comparativo de las teorías de daño acumulado por fatiga y predicción de la vida útil de componentes mecánicos aplicado a un eje ferroviario,” p. 99, 2017.
- [2] G. Dieter, *Metalurgia Mecanica*. Mexico: McGraw Hill, 1984.
- [3] C. L. Sandoval-Rodriguez, J. G. A. Villabona, C. G. Cárdenas-Arias, A. D. Rincon-Quintero, and B. E. Tarazona-Romero, “Characterization of the mechanical vibration signals associated with unbalance and misalignment in rotating machines, using the cepstrum transformation and the principal component analysis,” in *IOP Conference Series: Materials Science and Engineering*, 2020, p. 12057.
- [4] W. Chun-sheng, Z. Mu-sai, and W. Yu-zhu, “Research progresses on fatigue in steel bridges,” *J. Traffic Transp. Eng.*, vol. 24, no. 1, pp. 9–42, 2024.
- [5] Y. Kasper *et al.*, “Application of toughened epoxy-adhesives for strengthening of fatigue-damaged steel structures,” *Constr. Build. Mater.*, vol. 275, p. 121579, 2021.
- [6] Y. Yin, X. Niu, L. Han, Y. Lu, and K. Pu, “Study on ultra-low cycle fatigue of steel slit dampers,” in *Structures*, 2024, p. 106730.
- [7] H. Abdelbaset and Z. Zhu, “Behavior and fatigue life assessment of orthotropic steel decks: A state-of-the-art-review,” in *Structures*, 2024, p. 105957.
- [8] F. Suarez, “Análisis Del Proceso De Fractura En Materiales Estructurales Mediante El Uso Del Criterio De La Densidad De Energía De Deformación Y El Concepto De Material Equivalente,” 2019.
- [9] K. Cui, L. Xu, L. Li, and Y. Chi, “Mechanical performance of steel-polypropylene hybrid fiber reinforced concrete subject to uniaxial constant-amplitude cyclic compression: Fatigue behavior and unified fatigue equation,” *Compos. Struct.*, vol. 311, p. 116795, 2023.
- [10] F. Chen, H. Zhang, Z. Li, Y. Luo, X. Xiao, and Y. Liu, “Residual stresses effects on fatigue crack growth behavior of rib-to-deck double-sided welded joints in orthotropic steel decks,” *Adv. Struct. Eng.*, vol. 27, no. 1, pp. 35–50, 2024.
- [11] J. Antonio Echeverría, L. I. Negrín-Hernández I, E. A. Pérez-Ruiz II, R. I. Rodríguez-Marcial, and N. Cárdenas-Olivier III, “Quenching of SAE/AISI 1045 steel using reused oils as a cooling medium medium,” vol. 25, no. 1, pp. 1–6, 2021.
- [12] L. Toranzo, D. Fadruga, and N. Barrueta, “Selection of materials in the design process,” *A3manos*, vol. 7, no. 13. pp. 46–53, 2020.
- [13] Y. Ding, X.-W. Ye, H. Zhang, and X.-S. Zhang, “Fatigue life evolution of steel wire considering corrosion-fatigue coupling effect: Analytical model and application,” *Steel Compos. Struct.*, vol. 50, no. 3, pp. 363–374, 2024.
- [14] Y. Wang, C. Wang, and L. Duan, “Bonding and bolting angle reinforcement for distortion-induced fatigue in steel girder bridges,” *Thin-Walled Struct.*, vol. 166, p. 108027, 2021.
- [15] P. Romanowicz, B. Szybiński, and M. Wygoda, “Fracture Mechanism of Adhesive Layers in Fatigue-Loaded Steel Structures Reinforced by the CFRP Overlays,” *Appl. Sci.*, vol. 15, no. 7, p. 3435, 2025.
- [16] H. W. Lee, M. B. Djukic, and C. Basaran, “Modeling fatigue life and hydrogen embrittlement of bcc steel with unified mechanics theory,” *Int. J. Hydrogen Energy*, vol. 48, no. 54, pp. 20773–20803, 2023.

- [17] C. Huang, L. Li, N. Pichler, E. Ghafoori, L. Susmel, and L. Gardner, "Fatigue testing and analysis of steel plates manufactured by wire-arc directed energy deposition," *Addit. Manuf.*, vol. 73, p. 103696, 2023.
- [18] A. Parada, "Progressive fissure fatigue," *Apuntes*, vol. 5 Ed., 2002.
- [19] X. Wei, S. van der Zwaag, Z. Jia, C. Wang, and W. Xu, "On the use of transfer modeling to design new steels with excellent rotating bending fatigue resistance even in the case of very small calibration datasets," *Acta Mater.*, vol. 235, p. 118103, 2022.
- [20] G. Wang, Y. Ma, Z. Guo, H. Bian, L. Wang, and J. Zhang, "Fatigue life assessment of high-strength steel wires: Beach marks test and numerical investigation," *Constr. Build. Mater.*, vol. 323, p. 126534, 2022.
- [21] P. Wang *et al.*, "Effects of inclusion types on the high-cycle fatigue properties of high-strength steel," *Scr. Mater.*, vol. 206, p. 114232, 2022.
- [22] C. Xu *et al.*, "Effect of shot peening on the surface integrity and fatigue property of gear steel 16Cr3NiWMoVNB at room temperature," *Int. J. Fatigue*, vol. 172, p. 107668, 2023.
- [23] X. Xiao, H. Zhang, Z. Li, and F. Chen, "Effect of temperature on the fatigue life assessment of suspension bridge steel deck welds under dynamic vehicle loading," *Math. Probl. Eng.*, vol. 2022, no. 1, p. 7034588, 2022.
- [24] Tractermia, "Templado del acero y revenido."
- [25] H. Chen, S. Li, Y. Ren, X. Hou, H. Yang, and S. Zhang, "Thermo-mechanical fatigue behavior and microstructure evolution of 4Cr5Mo3V hot work die steel," *Int. J. Fatigue*, vol. 183, p. 108263, 2024.
- [26] C. G. Cárdenas-Arias, A. D. Rincón-Quintero, A. Santos-Jaimes, C. L. Sandoval-Rodriguez, D. F. Rojas-Gomez, and S. J. Ardila-Galvis, "Elasticity modulus variation of the AISI SAE 1045 steel subjected to corrosion process by chloride using tension test destructive," in *IOP Conference Series: Materials Science and Engineering*, 2020, p. 12059.
- [27] I. ASTM, "Standard Test Method for Strain-Controlled Fatigue Testing 1 E606," *ASTM Stand. E606*, vol. 92, no. 2004, pp. 1–16, 2013, doi: 10.1520/E0606-04E01.Copyright.
- [28] A. Bonilla Riveros, "Experimental design for rotary bending fatigue tests on low carbon steels (1000 series) for the materials laboratory of the Antonio Nariño University, Bucaramanga headquarters.," 2015.
- [29] I. ASTM, "ASTM E739 – 23," *Des. E 778 – 87 (Reapproved 2004)*, vol. i, no. Reapproved, pp. 3–5, 2018, doi: 10.1520/E0739-23.2.
- [30] W. W. D. Askeland, *Ciencia e Ingeniería de Materiales*, 7 ed. Mexico: Cengage Learning, 2017.
- [31] D. S. J. Rodríguez, "Diseño de una máquina para el laboratorio de tratamientos térmicos," pp. 1–23, 2016.
- [32] S. Founders, "Steel Casting Handbook: Design Rules and Data."
- [33] H. Jiménez, "Effect of Tempering Temperature on Microstructural, Crystallographic and Wear Resistance Properties of ASI / SAE 1045 Steel," vol. 26, no. 02, pp. 152–157, 2021.
- [34] S. Founders, "Hardenability and Heat Treatment," *Steel Castings Handbook*. pp. 24-1-24–42, 2022. doi: 10.31399/asm.tb.sch6.t68200327.
- [35] S. Quintana, "Diseño de un banco de pruebas de fatiga en flexión rotativa para evaluar el comportamiento

a cargas cíclicas,” *Sci. Tech.*, vol. 23, no. 3, pp. 324–333, 2018, doi: 10.22517/23447214.16891.